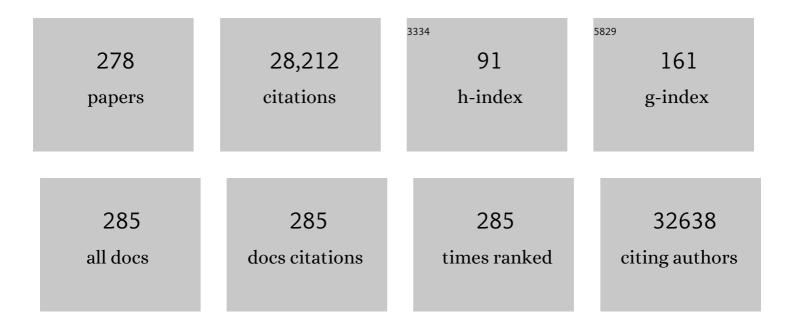
List of Publications by Year in descending order

Source: https://exaly.com/author-pdf/3647895/publications.pdf Version: 2024-02-01



Ін Снем

#	Article	IF	CITATIONS
1	Crumpled Nitrogenâ€Ðoped Graphene Nanosheets with Ultrahigh Pore Volume for Highâ€Performance Supercapacitor. Advanced Materials, 2012, 24, 5610-5616.	21.0	880
2	Constructing 2D Porous Graphitic C ₃ N ₄ Nanosheets/Nitrogenâ€Đoped Graphene/Layered MoS ₂ Ternary Nanojunction with Enhanced Photoelectrochemical Activity. Advanced Materials, 2013, 25, 6291-6297.	21.0	772
3	An Advanced Nitrogenâ€Doped Graphene/Cobaltâ€Embedded Porous Carbon Polyhedron Hybrid for Efficient Catalysis of Oxygen Reduction and Water Splitting. Advanced Functional Materials, 2015, 25, 872-882.	14.9	683
4	Reduced graphene oxide for room-temperature gas sensors. Nanotechnology, 2009, 20, 445502.	2.6	652
5	Enhanced Adsorptive Removal of Methyl Orange and Methylene Blue from Aqueous Solution by Alkali-Activated Multiwalled Carbon Nanotubes. ACS Applied Materials & Interfaces, 2012, 4, 5749-5760.	8.0	645
6	High-performance bi-functional electrocatalysts of 3D crumpled graphene–cobalt oxide nanohybrids for oxygen reduction and evolution reactions. Energy and Environmental Science, 2014, 7, 609-616.	30.8	605
7	Ultrahigh sensitivity and layer-dependent sensing performance of phosphorene-based gas sensors. Nature Communications, 2015, 6, 8632.	12.8	598
8	Nitrogenâ€Enriched Coreâ€Shell Structured Fe/Fe ₃ Câ€C Nanorods as Advanced Electrocatalysts for Oxygen Reduction Reaction. Advanced Materials, 2012, 24, 1399-1404.	21.0	517
9	Metalâ^'Organic Frameworkâ€Derived Nitrogenâ€Doped Coreâ€Shellâ€Structured Porous Fe/Fe ₃ C@C Nanoboxes Supported on Graphene Sheets for Efficient Oxygen Reduction Reactions. Advanced Energy Materials, 2014, 4, 1400337.	19.5	512
10	Metal–Organic-Framework-Derived Fe-N/C Electrocatalyst with Five-Coordinated Fe-N _{<i>x</i>} Sites for Advanced Oxygen Reduction in Acid Media. ACS Catalysis, 2017, 7, 1655-1663.	11.2	483
11	Graphene oxide and its reduction: modeling and experimental progress. RSC Advances, 2012, 2, 2643.	3.6	463
12	Specific Protein Detection Using Thermally Reduced Graphene Oxide Sheet Decorated with Gold Nanoparticleâ€Antibody Conjugates. Advanced Materials, 2010, 22, 3521-3526.	21.0	444
13	Green preparation of reduced graphene oxide for sensing and energy storage applications. Scientific Reports, 2014, 4, 4684.	3.3	433
14	Multilayered Si Nanoparticle/Reduced Graphene Oxide Hybrid as a Highâ€Performance Lithiumâ€Ion Battery Anode. Advanced Materials, 2014, 26, 758-764.	21.0	387
15	Plasma-enhanced chemical vapor deposition synthesis of vertically oriented graphene nanosheets. Nanoscale, 2013, 5, 5180.	5.6	357
16	Toward Practical Gas Sensing with Highly Reduced Graphene Oxide: A New Signal Processing Method To Circumvent Run-to-Run and Device-to-Device Variations. ACS Nano, 2011, 5, 1154-1164.	14.6	353
17	Gas detection using low-temperature reduced graphene oxide sheets. Applied Physics Letters, 2009, 94, .	3.3	346
18	Stabilizing MoS ₂ Nanosheets through SnO ₂ Nanocrystal Decoration for Highâ€Performance Gas Sensing in Air. Small, 2015, 11, 2305-2313.	10.0	333

#	Article	IF	CITATIONS
19	Oxygen reduction reaction catalysts used in microbial fuel cells for energy-efficient wastewater treatment: a review. Materials Horizons, 2016, 3, 382-401.	12.2	322
20	Two-dimensional nanomaterial-based field-effect transistors for chemical and biological sensing. Chemical Society Reviews, 2017, 46, 6872-6904.	38.1	316
21	Roomâ€Temperature Gas Sensing Based on Electron Transfer between Discrete Tin Oxide Nanocrystals and Multiwalled Carbon Nanotubes. Advanced Materials, 2009, 21, 2487-2491.	21.0	281
22	In Situ Confinement Pyrolysis Transformation of ZIFâ€8 to Nitrogenâ€Enriched Mesoâ€Microporous Carbon Frameworks for Oxygen Reduction. Advanced Functional Materials, 2016, 26, 8334-8344.	14.9	281
23	Perpendicularly Oriented MoSe ₂ /Graphene Nanosheets as Advanced Electrocatalysts for Hydrogen Evolution. Small, 2015, 11, 414-419.	10.0	276
24	Tuning gas-sensing properties of reduced graphene oxide using tin oxide nanocrystals. Journal of Materials Chemistry, 2012, 22, 11009.	6.7	274
25	Vertically Oriented Graphene Bridging Activeâ€Layer/Current ollector Interface for Ultrahigh Rate Supercapacitors. Advanced Materials, 2013, 25, 5799-5806.	21.0	270
26	Emerging energy and environmental applications of vertically-oriented graphenes. Chemical Society Reviews, 2015, 44, 2108-2121.	38.1	269
27	Enhancing Solar Cell Efficiencies through 1-D Nanostructures. Nanoscale Research Letters, 2009, 4, .	5.7	259
28	Strongly Coupled Ternary Hybrid Aerogels of N-deficient Porous Graphitic-C ₃ N ₄ Nanosheets/N-Doped Graphene/NiFe-Layered Double Hydroxide for Solar-Driven Photoelectrochemical Water Oxidation. Nano Letters, 2016, 16, 2268-2277.	9.1	256
29	Three-dimensional graphene-based composites for energy applications. Nanoscale, 2015, 7, 6924-6943.	5.6	241
30	Silicon nanotube anode for lithium-ion batteries. Electrochemistry Communications, 2013, 29, 67-70.	4.7	236
31	N-doped graphene/porous g-C3N4 nanosheets supported layered-MoS2 hybrid as robust anode materials for lithium-ion batteries. Nano Energy, 2014, 8, 157-164.	16.0	234
32	Alginate/graphene double-network nanocomposite hydrogel beads with low-swelling, enhanced mechanical properties, and enhanced adsorption capacity. Journal of Materials Chemistry A, 2016, 4, 10885-10892.	10.3	225
33	Hg(II) Ion Detection Using Thermally Reduced Graphene Oxide Decorated with Functionalized Gold Nanoparticles. Analytical Chemistry, 2012, 84, 4057-4062.	6.5	224
34	A room-temperature liquid metal-based self-healing anode for lithium-ion batteries with an ultra-long cycle life. Energy and Environmental Science, 2017, 10, 1854-1861.	30.8	219
35	Co3O4 nanoparticles embedded in nitrogen-doped porous carbon dodecahedrons with enhanced electrochemical properties for lithium storage and water splitting. Nano Energy, 2015, 12, 1-8.	16.0	210
36	Nickel oxide hollow microsphere for non-enzyme glucose detection. Biosensors and Bioelectronics, 2014, 54, 251-257.	10.1	208

#	Article	IF	CITATIONS
37	Field-effect transistor biosensors with two-dimensional black phosphorus nanosheets. Biosensors and Bioelectronics, 2017, 89, 505-510.	10.1	206
38	Nanocarbon-based gas sensors: progress and challenges. Journal of Materials Chemistry A, 2014, 2, 5573.	10.3	202
39	A General Approach to One-Pot Fabrication of Crumpled Graphene-Based Nanohybrids for Energy Applications. ACS Nano, 2012, 6, 7505-7513.	14.6	201
40	A 3D hybrid of layered MoS ₂ /nitrogen-doped graphene nanosheet aerogels: an effective catalyst for hydrogen evolution in microbial electrolysis cells. Journal of Materials Chemistry A, 2014, 2, 13795-13800.	10.3	198
41	Controllable Synthesis of Hollow Si Anode for Longâ€Cycleâ€Life Lithiumâ€Ion Batteries. Advanced Materials, 2014, 26, 4326-4332.	21.0	193
42	Carbon Nanotube with Chemically Bonded Graphene Leaves for Electronic and Optoelectronic Applications. Journal of Physical Chemistry Letters, 2011, 2, 1556-1562.	4.6	190
43	Amorphous MoS _x Cl _y electrocatalyst supported by vertical graphene for efficient electrochemical and photoelectrochemical hydrogen generation. Energy and Environmental Science, 2015, 8, 862-868.	30.8	183
44	Model of the Negative DC Corona Plasma: Comparison to the Positive DC Corona Plasma. Plasma Chemistry and Plasma Processing, 2003, 23, 83-102.	2.4	179
45	Strongly Coupled 3D Hybrids of Nâ€doped Porous Carbon Nanosheet/CoNi Alloyâ€Encapsulated Carbon Nanotubes for Enhanced Electrocatalysis. Small, 2015, 11, 5940-5948.	10.0	176
46	Direct Growth of Vertically-oriented Graphene for Field-Effect Transistor Biosensor. Scientific Reports, 2013, 3, 1696.	3.3	173
47	Metal Nitride/Graphene Nanohybrids: General Synthesis and Multifunctional Titanium Nitride/Graphene Electrocatalyst. Advanced Materials, 2011, 23, 5445-5450.	21.0	171
48	MOFâ€Based Metalâ€Dopingâ€Induced Synthesis of Hierarchical Porous CuN/C Oxygen Reduction Electrocatalysts for Zn–Air Batteries. Small, 2017, 13, 1700740.	10.0	170
49	Facile Oneâ€Pot, Oneâ€5tep Synthesis of a Carbon Nanoarchitecture for an Advanced Multifunctonal Electrocatalyst. Angewandte Chemie - International Edition, 2014, 53, 6496-6500.	13.8	169
50	Fast and Selective Room-Temperature Ammonia Sensors Using Silver Nanocrystal-Functionalized Carbon Nanotubes. ACS Applied Materials & Interfaces, 2012, 4, 4898-4904.	8.0	164
51	Graphene-based sensors for detection of heavy metals in water: a review. Analytical and Bioanalytical Chemistry, 2014, 406, 3957-3975.	3.7	163
52	One-step fabrication and capacitive behavior of electrochemical double layer capacitor electrodes using vertically-oriented graphene directly grown on metal. Carbon, 2012, 50, 4379-4387.	10.3	162
53	Patterning Vertically Oriented Graphene Sheets for Nanodevice Applications. Journal of Physical Chemistry Letters, 2011, 2, 537-542.	4.6	159
54	Semiconducting graphene: converting graphene from semimetal to semiconductor. Nanoscale, 2013, 5, 1353.	5.6	158

#	Article	IF	CITATIONS
55	A Hierarchical Tin/Carbon Composite as an Anode for Lithiumâ€lon Batteries with a Long Cycle Life. Angewandte Chemie - International Edition, 2015, 54, 1490-1493.	13.8	158
56	Transport, Analyte Detection, and Opto-Electronic Response of p-Type CuO Nanowires. Journal of Physical Chemistry C, 2010, 114, 2440-2447.	3.1	157
57	Metal Oxide/Carbide/Carbon Nanocomposites: In Situ Synthesis, Characterization, Calculation, and their Application as an Efficient Counter Electrode Catalyst for Dye‧ensitized Solar Cells. Advanced Energy Materials, 2013, 3, 1407-1412.	19.5	157
58	Synthesizing Nitrogen-Doped Activated Carbon and Probing its Active Sites for Oxygen Reduction Reaction in Microbial Fuel Cells. ACS Applied Materials & (1), 1), 1), 10, 2014, 6, 7464-7470.	8.0	157
59	Enhanced photovoltaic performance of perovskite CH ₃ NH ₃ PbI ₃ solar cells with freestanding TiO ₂ nanotube array films. Chemical Communications, 2014, 50, 6368-6371.	4.1	156
60	Ozone Production in the Positive DC Corona Discharge: Model and Comparison to Experiments. Plasma Chemistry and Plasma Processing, 2002, 22, 495-522.	2.4	155
61	A three-dimensionally interconnected carbon nanotube/layered MoS2 nanohybrid network for lithium ion battery anode with superior rate capacity and long-cycle-life. Nano Energy, 2015, 16, 10-18.	16.0	155
62	Controllable Synthesis and Tunable Photocatalytic Properties of Ti3+-doped TiO2. Scientific Reports, 2015, 5, 10714.	3.3	152
63	Surfactant assisted Ce–Fe mixed oxide decorated multiwalled carbon nanotubes and their arsenic adsorption performance. Journal of Materials Chemistry A, 2013, 1, 11355.	10.3	151
64	Confined phosphorus in carbon nanotube-backboned mesoporous carbon as superior anode material for sodium/potassium-ion batteries. Nano Energy, 2018, 52, 1-10.	16.0	148
65	Facile, noncovalent decoration of graphene oxide sheets with nanocrystals. Nano Research, 2009, 2, 192-200.	10.4	145
66	Rapid detection of single E. coli bacteria using a graphene-based field-effect transistor device. Biosensors and Bioelectronics, 2018, 110, 16-22.	10.1	144
67	TiO2 nanoparticles-decorated carbon nanotubes for significantly improved bioelectricity generation in microbial fuel cells. Journal of Power Sources, 2013, 234, 100-106.	7.8	136
68	Indium-doped SnO2 nanoparticle–graphene nanohybrids: simple one-pot synthesis and their selective detection of NO2. Journal of Materials Chemistry A, 2013, 1, 4462.	10.3	129
69	Nitrogen-doped graphene/CoNi alloy encased within bamboo-like carbon nanotube hybrids as cathode catalysts in microbial fuel cells. Journal of Power Sources, 2016, 307, 561-568.	7.8	128
70	Decorating anode with bamboo-like nitrogen-doped carbon nanotubes for microbial fuel cells. Electrochemistry Communications, 2012, 14, 71-74.	4.7	127
71	Modulating Gas Sensing Properties of CuO Nanowires through Creation of Discrete Nanosized p–n Junctions on Their Surfaces. ACS Applied Materials & Interfaces, 2012, 4, 4192-4199.	8.0	125
72	Controllable synthesis of silver nanoparticle-decorated reduced graphene oxide hybrids for ammonia detection. Analyst, The, 2013, 138, 2877.	3.5	125

#	Article	IF	CITATIONS
73	Growth of carbon nanowalls at atmospheric pressure for one-step gas sensor fabrication. Nanoscale Research Letters, 2011, 6, 202.	5.7	123
74	Magnetic carbon nanotubes synthesis by Fenton's reagent method and their potential application for removal of azo dye from aqueous solution. Journal of Colloid and Interface Science, 2012, 378, 175-183.	9.4	122
75	One-pot, large-scale synthesis of magnetic activated carbon nanotubes and their applications for arsenic removal. Journal of Materials Chemistry A, 2013, 1, 4662.	10.3	122
76	Title is missing!. Plasma Chemistry and Plasma Processing, 2002, 22, 199-224.	2.4	121
77	Understanding growth of carbon nanowalls at atmospheric pressure using normal glow discharge plasma-enhanced chemical vapor deposition. Carbon, 2011, 49, 1849-1858.	10.3	120
78	Enhanced Performance of Supported HfO ₂ Counter Electrodes for Redox Couples Used in Dye‣ensitized Solar Cells. ChemSusChem, 2014, 7, 442-450.	6.8	117
79	Enhanced adsorption removal of antibiotics from aqueous solutions by modified alginate/graphene double network porous hydrogel. Journal of Colloid and Interface Science, 2017, 507, 250-259.	9.4	115
80	Strategies for Improving the Performance of Sensors Based on Organic Fieldâ€Effect Transistors. Advanced Materials, 2018, 30, e1705642.	21.0	114
81	Field-Effect Transistor Biosensor for Rapid Detection of Ebola Antigen. Scientific Reports, 2017, 7, 10974.	3.3	112
82	Real-Time, Selective Detection of Pb ²⁺ in Water Using a Reduced Graphene Oxide/Gold Nanoparticle Field-Effect Transistor Device. ACS Applied Materials & Interfaces, 2014, 6, 19235-19241.	8.0	111
83	Nanomaterialâ€enabled Rapid Detection of Water Contaminants. Small, 2015, 11, 5336-5359.	10.0	108
84	Batch and column adsorption of methylene blue by graphene/alginate nanocomposite: Comparison of single-network and double-network hydrogels. Journal of Environmental Chemical Engineering, 2016, 4, 147-156.	6.7	106
85	Ultrasensitive Mercury Ion Detection Using DNA-Functionalized Molybdenum Disulfide Nanosheet/Gold Nanoparticle Hybrid Field-Effect Transistor Device. ACS Sensors, 2016, 1, 295-302.	7.8	103
86	A new reducing agent to prepare single-layer, high-quality reduced graphene oxide for device applications. Nanoscale, 2011, 3, 2849.	5.6	99
87	3D dual-confined sulfur encapsulated in porous carbon nanosheets and wrapped with graphene aerogels as a cathode for advanced lithium sulfur batteries. Nanoscale, 2016, 8, 8228-8235.	5.6	99
88	Binding Sn-based nanoparticles on graphene as the anode of rechargeable lithium-ion batteries. Journal of Materials Chemistry, 2012, 22, 3300.	6.7	97
89	Rational design of mesoporous NiFe-alloy-based hybrids for oxygen conversion electrocatalysis. Journal of Materials Chemistry A, 2015, 3, 7986-7993.	10.3	95
90	Hierarchical Nanohybrids with Porous CNT-Networks Decorated Crumpled Graphene Balls for Supercapacitors. ACS Applied Materials & Interfaces, 2014, 6, 9881-9889.	8.0	94

#	Article	IF	CITATIONS
91	Hydrothermal synthesis of vanadium nitride and modulation of its catalytic performance for oxygen reduction reaction. Nanoscale, 2014, 6, 9608.	5.6	93
92	Self-healing liquid metal nanoparticles encapsulated in hollow carbon fibers as a free-standing anode for lithium-ion batteries. Nano Energy, 2019, 62, 883-889.	16.0	93
93	NiO-Microflower Formed by Nanowire-weaving Nanosheets with Interconnected Ni-network Decoration as Supercapacitor Electrode. Scientific Reports, 2015, 5, 11919.	3.3	92
94	Ultrasensitive Quantum Dot Fluorescence quenching Assay for Selective Detection of Mercury Ions in Drinking Water. Scientific Reports, 2014, 4, 5624.	3.3	91
95	Ozone Production in the Negative DC Corona: The Dependence of Discharge Polarity. Plasma Chemistry and Plasma Processing, 2003, 23, 501-518.	2.4	90
96	Selective removal of lead ions through capacitive deionization: Role of ion-exchange membrane. Chemical Engineering Journal, 2019, 361, 1535-1542.	12.7	89
97	Porous Carbon Nanosheets Codoped with Nitrogen and Sulfur for Oxygen Reduction Reaction in Microbial Fuel Cells. ACS Applied Materials & Interfaces, 2015, 7, 18672-18678.	8.0	86
98	Ultrafast room temperature NH3 sensing with positively gated reduced graphene oxide field-effect transistors. Chemical Communications, 2011, 47, 7761.	4.1	85
99	Hierarchical vertically oriented graphene as a catalytic counter electrode in dye-sensitized solar cells. Journal of Materials Chemistry A, 2013, 1, 188-193.	10.3	85
100	Highly sensitive protein sensor based on thermally-reduced graphene oxide field-effect transistor. Nano Research, 2011, 4, 921-930.	10.4	84
101	Highly porous N-doped graphene nanosheets for rapid removal of heavy metals from water by capacitive deionization. Chemical Communications, 2017, 53, 881-884.	4.1	84
102	HF-free synthesis of Si/C yolk/shell anodes for lithium-ion batteries. Journal of Materials Chemistry A, 2018, 6, 2593-2599.	10.3	84
103	Ultratrace antibiotic sensing using aptamer/graphene-based field-effect transistors. Biosensors and Bioelectronics, 2019, 126, 664-671.	10.1	83
104	Carbon/iron-based nanorod catalysts for hydrogen production in microbial electrolysis cells. Nano Energy, 2012, 1, 751-756.	16.0	82
105	Exploring Adsorption and Reactivity of NH ₃ on Reduced Graphene Oxide. Journal of Physical Chemistry C, 2013, 117, 10698-10707.	3.1	82
106	Ultrasonic-assisted self-assembly of monolayer graphene oxide for rapid detection of Escherichia coli bacteria. Nanoscale, 2013, 5, 3620.	5.6	82
107	Graphene Coupled with Nanocrystals: Opportunities and Challenges for Energy and Sensing Applications. Journal of Physical Chemistry Letters, 2013, 4, 2441-2454.	4.6	80
108	Ultrasensitive Chemical Sensing through Facile Tuning Defects and Functional Groups in Reduced Graphene Oxide. Analytical Chemistry, 2014, 86, 7516-7522.	6.5	80

#	Article	IF	CITATIONS
109	One-pot, solid-phase synthesis of magnetic multiwalled carbon nanotube/iron oxide composites and their application in arsenic removal. Journal of Colloid and Interface Science, 2014, 434, 9-17.	9.4	80
110	Evidence of Nanocrystalline Semiconducting Graphene Monoxide during Thermal Reduction of Graphene Oxide in Vacuum. ACS Nano, 2011, 5, 9710-9717.	14.6	78
111	Rational design of carbon network cross-linked Si–SiC hollow nanosphere as anode of lithium-ion batteries. Nanoscale, 2014, 6, 342-351.	5.6	76
112	A high-performance catalyst support for methanol oxidation with graphene and vanadium carbonitride. Nanoscale, 2015, 7, 1301-1307.	5.6	75
113	Effect of relative humidity on electron distribution and ozone production by DC coronas in air. IEEE Transactions on Plasma Science, 2005, 33, 808-812.	1.3	74
114	Ag nanocrystal as a promoter for carbon nanotube-based room-temperature gas sensors. Nanoscale, 2012, 4, 5887.	5.6	71
115	Superior electrocatalysis for hydrogen evolution with crumpled graphene/tungsten disulfide/tungsten trioxide ternary nanohybrids. Nano Energy, 2018, 47, 66-73.	16.0	71
116	Facile Hydrothermal Synthesis of Nanostructured Hollow Iron–Cerium Alkoxides and Their Superior Arsenic Adsorption Performance. ACS Applied Materials & Interfaces, 2014, 6, 14016-14025.	8.0	69
117	The effect of Ag nanoparticle loading on the photocatalytic activity of TiO2 nanorod arrays. Chemical Physics Letters, 2010, 485, 171-175.	2.6	68
118	Surfactant-free synthesis of graphene-functionalized carbon nanotube film as a catalytic counter electrode in dye-sensitized solar cells. Journal of Power Sources, 2014, 247, 999-1004.	7.8	68
119	Straightforward fabrication of a highly branched graphene nanosheet array for a Li-ion battery anode. Journal of Materials Chemistry, 2012, 22, 15514.	6.7	67
120	Vertically oriented graphene sheets grown on metallic wires for greener corona discharges: lower power consumption and minimized ozone emission. Energy and Environmental Science, 2011, 4, 2525.	30.8	66
121	Easy solid-phase synthesis of pH-insensitive heterogeneous CNTs/FeS Fenton-like catalyst for the removal of antibiotics from aqueous solution. Journal of Colloid and Interface Science, 2015, 444, 24-32.	9.4	66
122	Facile construction of novel BiOBr/Bi12O17Cl2 heterojunction composites with enhanced photocatalytic performance. Journal of Colloid and Interface Science, 2020, 560, 21-33.	9.4	66
123	Nitrogen Vacancy Structure Driven Photoeletrocatalytic Degradation of 4-Chlorophenol Using Porous Graphitic Carbon Nitride Nanosheets. ACS Sustainable Chemistry and Engineering, 2018, 6, 6497-6506.	6.7	65
124	Facile Synthesis of Highly Dispersed Co ₃ O ₄ Nanoparticles on Expanded, Thin Black Phosphorus for a ppb-Level NO _{<i>x</i>} Gas Sensor. ACS Sensors, 2018, 3, 1576-1583.	7.8	65
125	"Brick-like―N-doped graphene/carbon nanotube structure forming three-dimensional films as high performance metal-free counter electrodes in dye-sensitized solar cells. Journal of Power Sources, 2015, 273, 1048-1055.	7.8	64
126	Self-Healing Liquid Metal and Si Composite as a High-Performance Anode for Lithium-Ion Batteries. ACS Applied Energy Materials, 2018, 1, 1395-1399.	5.1	64

#	Article	IF	CITATIONS
127	Graphene as a template and structural scaffold for the synthesis of a 3D porous bio-adsorbent to remove antibiotics from water. RSC Advances, 2015, 5, 27964-27969.	3.6	62
128	Nanocasted synthesis of ordered mesoporous cerium iron mixed oxide and its excellent performances for As(<scp>v</scp>) and Cr(<scp>vi</scp>) removal from aqueous solutions. Dalton Transactions, 2014, 43, 10767-10777.	3.3	59
129	MnO 2 -GO double-shelled sulfur (S@MnO 2 @GO) as a cathode for Li-S batteries with improved rate capability and cyclic performance. Journal of Power Sources, 2017, 356, 72-79.	7.8	58
130	Adsorption of ciprofloxacin onto graphene–soy protein biocomposites. New Journal of Chemistry, 2015, 39, 3333-3336.	2.8	57
131	Pulse-Driven Capacitive Lead Ion Detection with Reduced Graphene Oxide Field-Effect Transistor Integrated with an Analyzing Device for Rapid Water Quality Monitoring. ACS Sensors, 2017, 2, 1653-1661.	7.8	57
132	Controlled decoration of carbon nanotubes with nanoparticles. Nanotechnology, 2006, 17, 2891-2894.	2.6	55
133	Nitrogen-doped activated carbon as a metal free catalyst for hydrogen production in microbial electrolysis cells. RSC Advances, 2014, 4, 49161-49164.	3.6	55
134	Three-dimensional carbon-coated Si/rGO nanostructures anchored by nickel foam with carbon nanotubes for Li-ion battery applications. Nano Energy, 2015, 15, 679-687.	16.0	55
135	Strategies for Rational Design of Highâ€Power Lithiumâ€ion Batteries. Energy and Environmental Materials, 2021, 4, 19-45.	12.8	53
136	Understanding, discovery, and synthesis of 2D materials enabled by machine learning. Chemical Society Reviews, 2022, 51, 1899-1925.	38.1	53
137	3 D Singleâ€Walled Carbon Nanotube/Graphene Aerogels as Ptâ€Free Transparent Counter Electrodes for High Efficiency Dyeâ€Sensitized Solar Cells. ChemSusChem, 2014, 7, 3304-3311.	6.8	52
138	Metallic CoS ₂ nanowire electrodes for high cycling performance supercapacitors. Nanotechnology, 2015, 26, 494001.	2.6	52
139	One-pot synthesis of high-performance Co/graphene electrocatalysts for glucose fuel cells free of enzymes and precious metals. Chemical Communications, 2015, 51, 9354-9357.	4.1	52
140	Ultrafast hydrogen sensing through hybrids of semiconducting single-walled carbon nanotubes and tin oxide nanocrystals. Nanoscale, 2012, 4, 1275.	5.6	51
141	A simple and versatile mini-arc plasma source for nanocrystal synthesis. Journal of Nanoparticle Research, 2007, 9, 203-213.	1.9	50
142	Nitrogen-doped graphene–vanadium carbide hybrids as a high-performance oxygen reduction reaction electrocatalyst support in alkaline media. Journal of Materials Chemistry A, 2013, 1, 13404.	10.3	50
143	Phosphorus/Carbon Composite Anode for Potassium-Ion Batteries: Insights into High Initial Coulombic Efficiency and Superior Cyclic Performance. ACS Sustainable Chemistry and Engineering, 2018, 6, 16308-16314.	6.7	50
144	Free standing TiO2 nanotube array electrodes with an ultra-thin Al2O3 barrier layer and TiCl4 surface modification for highly efficient dye sensitized solar cells. Nanoscale, 2013, 5, 10438.	5.6	49

#	Article	IF	CITATIONS
145	Graphene-Based Materials for Photoanodes in Dye-Sensitized Solar Cells. Frontiers in Energy Research, 2015, 3, .	2.3	49
146	Enzymeless Glucose Detection Based on CoO/Graphene Microsphere Hybrids. Electroanalysis, 2014, 26, 1326-1334.	2.9	48
147	Direct Oxidation Growth of CuO Nanowires from Copper-Containing Substrates. Journal of Nanomaterials, 2008, 2008, 1-7.	2.7	46
148	Additive manufacturing and applications of nanomaterial-based sensors. Materials Today, 2021, 48, 135-154.	14.2	46
149	Tailoring MOF-derived porous carbon nanorods confined red phosphorous for superior potassium-ion storage. Nano Energy, 2021, 83, 105797.	16.0	44
150	Effects of N and F doping on structure and photocatalytic properties of anatase TiO2 nanoparticles. RSC Advances, 2013, 3, 16657.	3.6	43
151	Healing of reduced graphene oxide with methaneÂ+ hydrogen plasma. Carbon, 2017, 120, 274-280.	10.3	43
152	Rapid detection of nutrients with electronic sensors: a review. Environmental Science: Nano, 2018, 5, 837-862.	4.3	41
153	Real-time electronic sensor based on black phosphorus/Au NPs/DTT hybrid structure: Application in arsenic detection. Sensors and Actuators B: Chemical, 2018, 257, 214-219.	7.8	41
154	Real-time and selective detection of nitrates in water using graphene-based field-effect transistor sensors. Environmental Science: Nano, 2018, 5, 1990-1999.	4.3	41
155	Single-walled carbon nanotube field-effect transistors with graphene oxide passivation for fast, sensitive, and selective proteindetection. Biosensors and Bioelectronics, 2013, 42, 186-192.	10.1	40
156	Lanthanum and Neodymium Doped Barium Ferrite-TiO2/MCNTs/poly(3-methyl thiophene) Composites with Nest Structures: Preparation, Characterization and Electromagnetic Microwave Absorption Properties. Scientific Reports, 2016, 6, 20496.	3.3	40
157	Specific biosensing using carbon nanotubes functionalized with gold nanoparticle–antibody conjugates. Carbon, 2010, 48, 479-486.	10.3	39
158	Improved Cyclic Performance of Si Anodes for Lithium-Ion Batteries by Forming Intermetallic Interphases between Si Nanoparticles and Metal Microparticles. ACS Applied Materials & Interfaces, 2013, 5, 11965-11970.	8.0	39
159	Selectivity of Per- and Polyfluoroalkyl Substance Sensors and Sorbents in Water. ACS Applied Materials & Interfaces, 2021, 13, 60789-60814.	8.0	39
160	Real-time detection of mercury ions in water using a reduced graphene oxide/DNA field-effect transistor with assistance of a passivation layer. Sensing and Bio-Sensing Research, 2015, 5, 97-104.	4.2	38
161	Decorating in situ ultrasmall tin particles on crumpled N-doped graphene for lithium-ion batteries with a long life cycle. Journal of Power Sources, 2016, 328, 482-491.	7.8	38
162	Electrospinning pectin-based nanofibers: a parametric and cross-linker study. Applied Nanoscience (Switzerland), 2018, 8, 33-40.	3.1	38

#	Article	IF	CITATIONS
163	Nitrogen-boron Dipolar-doped Nanocarbon as a High-efficiency Electrocatalyst for Oxygen Reduction Reaction. Electrochimica Acta, 2016, 222, 481-487.	5.2	37
164	Short-circuit diffusion growth of long bi-crystal CuO nanowires. Chemical Physics Letters, 2011, 504, 41-45.	2.6	36
165	A TiO ₂ nanotube network electron transport layer for high efficiency perovskite solar cells. Physical Chemistry Chemical Physics, 2017, 19, 4956-4961.	2.8	33
166	Nanoscale Discharge Electrode for Minimizing Ozone Emission from Indoor Corona Devices. Environmental Science & Technology, 2010, 44, 6337-6342.	10.0	32
167	Facile synthesis of three-dimensional graphene–soy protein aerogel composites for tetracycline adsorption. Desalination and Water Treatment, 2016, 57, 9510-9519.	1.0	32
168	Organometallic Precursor-Derived SnO ₂ /Sn-Reduced Graphene Oxide Sandwiched Nanocomposite Anode with Superior Lithium Storage Capacity. ACS Applied Materials & Interfaces, 2018, 10, 26170-26177.	8.0	32
169	Fe–Mn Mixed Oxide Catalysts Synthesized by One-Step Urea-Precipitation Method for the Selective Catalytic Reduction of NO x with NH3 at Low Temperatures. Catalysis Letters, 2018, 148, 227-234.	2.6	31
170	One-step, continuous synthesis of a spherical Li4Ti5O12/graphene composite as an ultra-long cycle life lithium-ion battery anode. NPG Asia Materials, 2015, 7, e224-e224.	7.9	30
171	Novel bioprinting method using a pectin based bioink. Technology and Health Care, 2017, 25, 651-655.	1.2	30
172	Temperature-dependent Crystallization of MoS2 Nanoflakes on Graphene Nanosheets for Electrocatalysis. Nanoscale Research Letters, 2017, 12, 479.	5.7	30
173	Resonance-Frequency Modulation for Rapid, Point-of-Care Ebola-Glycoprotein Diagnosis with a Graphene-Based Field-Effect Biotransistor. Analytical Chemistry, 2018, 90, 14230-14238.	6.5	30
174	Sensitive field-effect transistor sensors with atomically thin black phosphorus nanosheets. Nanoscale, 2020, 12, 1500-1512.	5.6	30
175	A facile one-pot method for synthesis of low-cost magnetic carbon nanotubes and their applications for dye removal. New Journal of Chemistry, 2012, 36, 1940.	2.8	28
176	Enhancing the performance of free-standing TiO2 nanotube arrays based dye-sensitized solar cells via ultraprecise control of the nanotube wall thickness. Journal of Power Sources, 2013, 240, 503-509.	7.8	28
177	Self-regenerative adsorbent based on the cross-linking chitosan for adsorbing and mineralizing azo dye. RSC Advances, 2014, 4, 5518.	3.6	28
178	Novel hybrid Si film/carbon nanofibers as anode materials in lithium-ion batteries. Journal of Materials Chemistry A, 2015, 3, 1947-1952.	10.3	28
179	Ultrasensitive detection of orthophosphate ions with reduced graphene oxide/ferritin field-effect transistor sensors. Environmental Science: Nano, 2017, 4, 856-863.	4.3	28
180	Multifunctional UV and Gas Sensors Based on Vertically Nanostructured Zinc Oxide: Volume Versus Surface Effect. Sensors, 2019, 19, 2061.	3.8	28

#	Article	IF	CITATIONS
181	Optimized CdS quantum dot-sensitized solar cell performance through atomic layer deposition of ultrathin TiO2 coating. RSC Advances, 2012, 2, 7843.	3.6	27
182	Highly sensitive room temperature carbon monoxide detection using SnO ₂ nanoparticle-decorated semiconducting single-walled carbon nanotubes. Nanotechnology, 2013, 24, 025503.	2.6	27
183	RIPENING OF SILVER NANOPARTICLES ON CARBON NANOTUBES. Nano, 2007, 02, 149-156.	1.0	26
184	Selective Deposition of CdSe Nanoparticles on Reduced Graphene Oxide to Understand Photoinduced Charge Transfer in Hybrid Nanostructures. ACS Applied Materials & Interfaces, 2011, 3, 2703-2709.	8.0	25
185	CNT@TiO2 nanohybrids for high-performance anode of lithium-ion batteries. Nanoscale Research Letters, 2013, 8, 499.	5.7	25
186	Fabrication of hierarchical core–shell Au@ZnO heteroarchitectures initiated by heteroseed assembly for photocatalytic applications. Journal of Colloid and Interface Science, 2014, 418, 171-177.	9.4	25
187	Electrochemical exfoliation of ultrathin ternary molybdenum sulfoselenide nanosheets to boost the energy-efficient hydrogen evolution reaction. Nanoscale, 2019, 11, 16200-16207.	5.6	25
188	A novel gas sensor based on porous α-Ni(OH) ₂ ultrathin nanosheet/reduced graphene oxide composites for room temperature detection of NO _x . New Journal of Chemistry, 2016, 40, 4678-4686.	2.8	24
189	Graphene-based electronic biosensors. Journal of Materials Research, 2017, 32, 2954-2965.	2.6	24
190	A simplified formulation of wire-plate corona discharge in air: Application to the ion wind simulation. Journal of Electrostatics, 2018, 92, 54-65.	1.9	24
191	Wastewater-Based Epidemiology for Managing the COVID-19 Pandemic. ACS ES&T Water, 2021, 1, 1352-1362.	4.6	24
192	Novel Hybrid Carbon Nanofiber/Highly Branched Graphene Nanosheet for Anode Materials in Lithium-Ion Batteries. ACS Applied Materials & Interfaces, 2014, 6, 18590-18596.	8.0	23
193	Vertically-Oriented Graphene. , 2015, , .		23
194	Improving cyclic performance of Si anode for lithium-ion batteries by forming an intermetallic skin. RSC Advances, 2015, 5, 38660-38664.	3.6	22
195	Calcium-oligochitosan-pectin microcarrier for colonic drug delivery. Pharmaceutical Development and Technology, 2020, 25, 260-265.	2.4	22
196	Directly Anchoring Highly Dispersed Copper Sites on Nitrogenâ€Đoped Carbon for Enhanced Oxygen Reduction Electrocatalysis. ChemElectroChem, 2018, 5, 1822-1826.	3.4	21
197	A facile one-pot method for synthesis of low-cost iron oxide/activated carbon nanotubeelectrode materials for lithium-ion batteries. Dalton Transactions, 2013, 42, 1356-1359.	3.3	20
198	From phosphorus nanorods/C to yolk–shell P@hollow C for potassium-ion batteries: high capacity with stable cycling performance. Journal of Materials Chemistry A, 2020, 8, 7641-7646.	10.3	20

#	Article	IF	CITATIONS
199	Instantaneous Reduction of Graphene Oxide Paper for Supercapacitor Electrodes with Unimpeded Liquid Permeation. Journal of Physical Chemistry C, 2014, 118, 13493-13502.	3.1	19
200	Coating carbon nanotubes with colloidal nanocrystals by combining an electrospray technique with directed assembly using an electrostatic field. Nanotechnology, 2008, 19, 455610.	2.6	18
201	Development of a Microscale Red Blood Cell-Shaped Pectin-Oligochitosan Hydrogel System Using an Electrospray-Vibration Method: Preparation and Characterization. Journal of Applied Biomaterials and Functional Materials, 2015, 13, 326-331.	1.6	18
202	Structure sensitivity of selective catalytic reduction of NO with propylene over Cu-doped Ti0.5Zr0.5O2â^ catalysts. Applied Catalysis B: Environmental, 2015, 165, 519-528.	20.2	18
203	In Operando Impedance Spectroscopic Analysis on NiO–WO ₃ Nanorod Heterojunction Random Networks for Room-Temperature H ₂ S Detection. ACS Omega, 2018, 3, 18685-18693.	3.5	18
204	Design of a Novel Oxygen Therapeutic Using Polymeric Hydrogel Microcapsules Mimicking Red Blood Cells. Pharmaceutics, 2019, 11, 583.	4.5	18
205	The growth mechanism of single-walled carbon nanotubes with a controlled diameter. Physica E: Low-Dimensional Systems and Nanostructures, 2012, 44, 2032-2040.	2.7	17
206	A Novel Redâ€Bloodâ€Cellâ€Shaped Pectinâ€Oligochitosan Hydrogel System. Particle and Particle Systems Characterization, 2014, 31, 955-959.	2.3	17
207	Semi-quantitative design of black phosphorous field-effect transistor sensors for heavy metal ion detection in aqueous media. Molecular Systems Design and Engineering, 2019, 4, 491-502.	3.4	17
208	Iron Oxide Supported Sulfhydrylâ€Functionalized Multiwalled Carbon Nanotubes for Removal of Arsenite from Aqueous Solution. ChemPlusChem, 2015, 80, 740-748.	2.8	16
209	An amperometric glucose enzyme biosensor based on porous hexagonal boron nitride whiskers decorated with Pt nanoparticles. RSC Advances, 2016, 6, 92748-92753.	3.6	16
210	Numerical modelling of ozone production in a wire–cylinder corona discharge and comparison with a wire–plate corona discharge. Journal Physics D: Applied Physics, 2009, 42, 035202.	2.8	15
211	Controllable photoelectron transfer in CdSe nanocrystal–carbon nanotube hybrid structures. Nanoscale, 2012, 4, 742-746.	5.6	15
212	Effects of ultrasonic radiation on induction period and nucleation kinetics of sodium sulfate. Korean Journal of Chemical Engineering, 2014, 31, 807-811.	2.7	15
213	Investigation of NO 2 adsorption on reduced graphene oxide. Chemical Physics Letters, 2015, 622, 86-91.	2.6	15
214	Field-Effect Transistor Based on Percolation Network of Reduced Graphene Oxide for Real-Time ppb-Level Detection of Lead Ions in Water. ECS Journal of Solid State Science and Technology, 2020, 9, 115012.	1.8	15
215	Synthesis, assembly, and characterization of Si nanocrystals and Si nanocrystal–carbon nanotube hybrid structures. Nanotechnology, 2008, 19, 265705.	2.6	14
216	A Generic Approach to Coat Carbon Nanotubes With Nanoparticles for Potential Energy Applications. Journal of Heat Transfer, 2008, 130, .	2.1	14

#	Article	IF	CITATIONS
217	Determination of metastable zone width and the primary nucleation kinetics of sodium sulfate. Theoretical Foundations of Chemical Engineering, 2015, 49, 869-876.	0.7	14
218	Stability improvement and characterization of bioprinted pectin-based scaffold. Journal of Applied Biomaterials and Functional Materials, 2019, 17, 228080001880710.	1.6	14
219	A Hybrid Model to Predict Electron and Ion Distributions in Entire Interelectrode Space of a Negative Corona Discharge. IEEE Transactions on Plasma Science, 2012, 40, 421-428.	1.3	13
220	BaFe12O19-chitosan Schiff-base Ag (I) complexes embedded in carbon nanotube networks for high-performance electromagnetic materials. Scientific Reports, 2015, 5, 12544.	3.3	13
221	Porous carbon and Prussian blue composite: A highly sensitive electrochemical platform for glucose biosensing. Sensing and Bio-Sensing Research, 2017, 14, 47-53.	4.2	13
222	Gas Sensors Based on Tin Oxide Nanoparticles Synthesized from a Mini-Arc Plasma Source. Journal of Nanomaterials, 2006, 2006, 1-7.	2.7	12
223	Si omposite Anode for Lithiumâ€ŀon Batteries with High Initial Coulombic Efficiency. Energy Technology, 2013, 1, 305-308.	3.8	12
224	Design of pectin-based bioink containing bioactive agent-loaded microspheres for bioprinting. Biomedical Physics and Engineering Express, 2019, 5, 067004.	1.2	12
225	Zero-wastewater capacitive deionization: selective removal of heavy metal ions in tap water assisted by phosphate ions. Environmental Science: Nano, 2019, 6, 3225-3231.	4.3	12
226	Ultrasensitive sensors based on aluminum oxide-protected reduced graphene oxide for phosphate ion detection in real water. Molecular Systems Design and Engineering, 2020, 5, 936-942.	3.4	12
227	Graphene-oxide loading on natural zeolite particles for enhancement of adsorption properties. RSC Advances, 2020, 10, 4589-4597.	3.6	12
228	One-dimensional tungsten oxide growth through a grain-by-grain buildup process. Chemical Physics Letters, 2010, 485, 64-68.	2.6	11
229	Decoration of vertical graphene with aerosol nanoparticles for gas sensing. Journal Physics D: Applied Physics, 2015, 48, 314008.	2.8	11
230	Hybrid Electrocatalysis: An Advanced Nitrogenâ€Đoped Graphene/Cobaltâ€Embedded Porous Carbon Polyhedron Hybrid for Efficient Catalysis of Oxygen Reduction and Water Splitting (Adv. Funct. Mater.) Tj ETQq0) 0 04r.g BT	/Oværlock 10
231	Quantitative analysis of the synergistic effect of Au nanoparticles on SnO ₂ –rGO nanocomposites for room temperature hydrogen sensing. Physical Chemistry Chemical Physics, 2021, 23, 2377-2383.	2.8	11
232	Molecular Engineering of 2D Nanomaterial Fieldâ€Effect Transistor Sensors: Fundamentals and Translation across the Innovation Spectrum. Advanced Materials, 2022, 34, e2106975.	21.0	11
233	Influence of partial substitution of Mo for Cr on structure and hydrogen storage characteristics of non-stoichiometric Laves phase TiCrB0.9 alloy. International Journal of Hydrogen Energy, 2013, 38, 11955-11963.	7.1	10
234	Dimensional Analysis of Detrimental Ozone Generation by Negative Wire-to-Plate Corona Discharge in Both Dry and Humid Air. Ozone: Science and Engineering, 2013, 35, 31-37.	2.5	10

#	Article	IF	CITATIONS
235	Graphene Supercapacitors: Vertically Oriented Graphene Bridging Active-Layer/Current-Collector Interface for Ultrahigh Rate Supercapacitors (Adv. Mater. 40/2013). Advanced Materials, 2013, 25, 5798-5798.	21.0	10
236	Remote Floating-Gate Field-Effect Transistor with 2-Dimensional Reduced Graphene Oxide Sensing Layer for Reliable Detection of SARS-CoV-2 Spike Proteins. ACS Applied Materials & Interfaces, 2022, 14, 24187-24196.	8.0	10
237	Chemical Vapor Deposition of Silicon Dioxide by Direct-Current Corona Discharges in Dry Air Containing Octamethylcyclotetrasiloxane Vapor: Measurement of the Deposition Rate. Plasma Chemistry and Plasma Processing, 2004, 24, 169-188.	2.4	9
238	Design of Artificial Red Blood Cells using Polymeric Hydrogel Microcapsules: Hydrogel Stability Improvement and Polymer Selection. International Journal of Artificial Organs, 2016, 39, 518-523.	1.4	9
239	Impedimetric phosphorene field-effect transistors for rapid detection of lead ions. Nanotechnology, 2018, 29, 375501.	2.6	9
240	A redox-active organic cation for safer high energy density Li-ion batteries. Journal of Materials Chemistry A, 2020, 8, 17156-17162.	10.3	9
241	Maximizing Solar Energy Utilization through Multicriteria Pareto Optimization of Energy Harvesting and Regulating Smart Windows. Cell Reports Physical Science, 2020, 1, 100108.	5.6	9
242	Note: Continuous synthesis of uniform vertical graphene on cylindrical surfaces. Review of Scientific Instruments, 2011, 82, 086116.	1.3	8
243	Nitrogen-Enriched Core-Shell Structured Fe/Fe3C-C Nanorods as Advanced Electrocatalysts for Oxygen Reduction Reaction (Adv. Mater. 11/2012). Advanced Materials, 2012, 24, 1398-1398.	21.0	8
244	Tailoring nanomaterial products through electrode material and oxygen partial pressure in a mini-arc plasma reactor. Journal of Nanoparticle Research, 2012, 14, 1.	1.9	7
245	Hollow TiO ₂ as an Anode for Lithium Ion Batteries: Synthesis and In Situ Visualization of State of Charge. Advanced Electronic Materials, 2015, 1, 1500256.	5.1	7
246	Diameter-dependent thermal-oxidative stability of single-walled carbon nanotubes synthesized by a floating catalytic chemical vapor deposition method. Applied Surface Science, 2011, 257, 10471-10476.	6.1	6
247	Novel hybrid Si film/highly branched graphene nanosheets for anode materials in lithium-ion batteries. Journal Physics D: Applied Physics, 2019, 52, 345201.	2.8	6
248	A Global Model of Chemical Vapor Deposition of Silicon Dioxide by Direct-Current Corona Discharges in Dry Air Containing Octamethylcyclotetrasiloxane Vapor. Plasma Chemistry and Plasma Processing, 2004, 24, 511-535.	2.4	5
249	Carbon-nanotube-assisted transmission electron microscopy characterization of aerosol nanoparticles. Journal of Aerosol Science, 2009, 40, 180-184.	3.8	5
250	Effect of Angle of Attack on the Performance of an Airborne Counterflow Virtual Impactor. Aerosol Science and Technology, 2005, 39, 485-491.	3.1	4
251	Carbon Nanotube-Nanoparticle Hybrid Structures. , 2010, , .		4
252	Hydrogen Evolution: Perpendicularly Oriented MoSe ₂ /Graphene Nanosheets as Advanced Electrocatalysts for Hydrogen Evolution (Small 4/2015). Small, 2015, 11, 508-508.	10.0	4

#	Article	IF	CITATIONS
253	Enhancing Cyclic Performance and Rate Capability of Li ₄ Ti ₅ O ₁₂ for Lithiumâ€lon Batteries through Thin Carbon Coating. ChemistrySelect, 2018, 3, 10792-10798.	1.5	4
254	Hybrid Modeling and Sensitivity Analysis on Reduced Graphene Oxide Field-Effect Transistor. IEEE Nanotechnology Magazine, 2021, 20, 404-416.	2.0	4
255	Biosynthesis of silver nanoparticles using upland cress: purification, characterisation, and antimicrobial activity. Micro and Nano Letters, 2020, 15, 110-113.	1.3	4
256	The Properties of Vertically-Oriented Graphene. , 2015, , 11-18.		4
257	PECVD Synthesis of Vertically-Oriented Graphene: Mechanism and Plasma Sources. , 2015, , 19-34.		3
258	Challenge-driven printing strategies toward high-performance solid-state lithium batteries. Journal of Materials Chemistry A, 2022, 10, 2601-2617.	10.3	3
259	Absorption Properties of Hybrid SnO2 Nanocrystal-Carbon Nanotube Structures. Journal of Electronic Materials, 2008, 37, 1686-1690.	2.2	2
260	Electrocatalysis: Strongly Coupled 3D Hybrids of N-doped Porous Carbon Nanosheet/CoNi Alloy-Encapsulated Carbon Nanotubes for Enhanced Electrocatalysis (Small 44/2015). Small, 2015, 11, 5939-5939.	10.0	2
261	PECVD Synthesis of Vertically-OrientedÂGraphene: Precursor and Temperature Effects. , 2015, , 35-54.		2
262	Protein Viability on Au Nanoparticles during an Electrospray and Electrostatic-Force-Directed Assembly Process. Journal of Nanomaterials, 2010, 2010, 1-6.	2.7	1
263	DC and Microwave Plasmas for Synthesis of Vertically Oriented Graphene. IEEE Transactions on Plasma Science, 2014, 42, 2796-2797.	1.3	1
264	Vertically-Oriented Graphene for Sensing and Environmental Applications. , 2015, , 67-77.		1
265	Vertically-Oriented Graphene for Supercapacitors. , 2015, , 79-95.		1
266	Interfacial charge transport behavior and thermal profiles of vertically oriented grapheneâ€bridged supercapacitors. Physica Status Solidi (B): Basic Research, 2017, 254, 1600804.	1.5	1
267	Electrocatalysts: MOFâ€Based Metalâ€Dopingâ€Induced Synthesis of Hierarchical Porous CuN/C Oxygen Reduction Electrocatalysts for Zn–Air Batteries (Small 30/2017). Small, 2017, 13, .	10.0	1
268	Spatial distribution quantification and control of ink flakes in reduced graphene oxide FET inkjet printing. Procedia Manufacturing, 2019, 34, 19-25.	1.9	1
269	Statistical Modeling and Analysis of k-Layer Coverage of Two-Dimensional Materials in Inkjet Printing Processes. Technometrics, 2021, 63, 410-420.	1.9	1
270	Design and Stability Improvement of Pectin-Based Red Blood Cell-Mimicking Microcapsules for Oxygen Therapeutics. Journal of Biomedical Nanotechnology, 2021, 17, 1798-1805.	1.1	1

#	Article	IF	CITATIONS
271	Landmark-embedded Gaussian process with applications for functional data modeling. IISE Transactions, 0, , 1-14.	2.4	1
272	Effect of relative humidity on electron distribution and ozone production by DC coronas in air. , 0, , .		0
273	Gas Sensors: Room-Temperature Gas Sensing Based on Electron Transfer between Discrete Tin Oxide Nanocrystals and Multiwalled Carbon Nanotubes (Adv. Mater. 24/2009). Advanced Materials, 2009, 21, NA-NA.	21.0	0
274	Hydrogels: A Novel Red-Blood-Cell-Shaped Pectin-Oligochitosan Hydrogel System (Part. Part. Syst.) Tj ETQqO 0 0	rgBT /Over 2.3	lock 10 Tf 50

275	Lithium-Ion Batteries: Hollow TiO2 as an Anode for Lithium Ion Batteries: Synthesis and In Situ Visualization of State of Charge (Adv. Electron. Mater. 12/2015). Advanced Electronic Materials, 2015, 1,	5.1	0
276	Atmospheric PECVD Growth of Vertically-OrientedÂGraphene. , 2015, , 55-65.		0
277	Vertically-Oriented Graphene for Other Energy Storage and Conversion Applications. , 2015, , 97-108.		0
278	Interfacial charge transport behavior and thermal profiles of vertically oriented grapheneâ€bridged supercapacitors (Phys. Status Solidi B 6/2017). Physica Status Solidi (B): Basic Research, 2017, 254, 1770232.	1.5	0